Cerebral Cortex, 2018; 1–12

doi: 10.1093/cercor/bhy140
Original Article

ORIGINAL ARTICLE

Altered Cortical and Hippocampal Excitability in TgF344-AD Rats Modeling Alzheimer's Disease Pathology

Milan Stoiljkovic, Craig Kelley, Bernardo Stutz, Tamas L. Horvath and Mihály Hajós

Department of Comparative Medicine, Yale University School of Medicine, New Haven, CT 06510, USA

Address correspondence to Milan Stoiljkovic, Tamas L. Horvath, Mihály Hajós, Department of Comparative Medicine, Yale University School of Medicine, 310 Cedar St., New Haven, CT 06510, USA. Email: milan.stoiljkovic@yale.edu (M.S.), tamas.horvath@yale.edu (T.L.H.), mihaly.hajos@yale.edu (M.H.)

Abstract

Current findings suggest that accumulation of amyloid-β (Aβ) and hyperphosphorylated tau in the brain disrupt synaptic function in hippocampal–cortical neuronal networks leading to impairment in cognitive and affective functions in Alzheimer's disease (AD). Development of new disease-modifying AD drugs are challenging due to the lack of predictive animal models and efficacy assays. In the present study we recorded neural activity in TgF344-AD rats, a transgenic model with a full array of AD pathological features, including age-dependent Aβ accumulation, tauopathy, neuronal loss, and cognitive impairments. Under urethane anesthesia, TgF344-AD rats showed significant age-dependent decline in brainstem-elicited hippocampal theta oscillation and decreased theta-phase gamma-amplitude coupling comparing to their age-matched wild-type counterparts. In freely-behaving condition, the power of hippocampal theta oscillation and gamma power during sharp-wave ripples were significantly lower in TgF344-AD rats. Additionally, these rats showed impaired coherence in both intercortical and hippocampal–cortical network dynamics, and increased incidence of paroxysmal high-voltage spindles, which occur during awake, behaviorally quiescent state. TgF344-AD rats demonstrated impairments in sensory processing, having diminished auditory gating and 40-Hz auditory evoked steady-state response. The observed differences in neurophysiological activities in TgF344-AD rats, which mirror several abnormalities described in AD patients, may be used as promising markers to monitor disease-modifying therapies.

Key words: Alzheimer's disease, high-voltage spindles, sensory processing, TgF344-AD, theta oscillation

Introduction

Understanding the neural basis of cognitive deficits, a core feature of Alzheimer's disease (AD), is of ultimate importance for identifying new viable biomarkers and developing disease-modifying therapies. Although currently used AD biomarkers, such as cerebrospinal fluid amyloid-β (Aβ) and tau, are suitable for establishing diagnosis, they are not reliable predictors for progression of cognitive impairments. Therefore, novel biomarkers detecting early neuronal dysfunctions associated with cognitive impairment are highly needed. Transgenic animals capturing certain aspects of AD pathology could be used to explore potential signs of disease progression. A recently developed transgenic rat model (TgF344-AD) expressing mutant human amyloid precursor protein (APPswe) and presenilin 1 (PS1ΔE9) genes, shows several aspects of AD pathology, including age-dependent cerebral amyloidosis, tauopathy, gliosis, apoptotic loss of neurons in the cerebral cortex and hippocampus, and cognitive disturbance (Cohen et al. 2013). Although some pathological changes occurred relative early in these rats (from 6 months), their cognitive decline was not observed until

they reach 12–15 months of age. In the present study, we evaluated neurophysiological signals in wild-type (WT) Fisher and TgF344-AD rats from 6 to 12 months of age.

The integrity of neuronal function in WT and TgF344-AD rats was investigated both under anesthesia and in freely-behaving condition. Our previous studies on Aβ overproducing APP/PS1 and 5xFAD mice, as well as on tau transgenic Tg4510 mice showed clear dysfunction in hippocampal network oscillation under urethane anesthesia (Scott et al. 2012, 2016; Stoiljkovic et al. 2016). In Aβ overproducing APP/PS1 mice, an age-dependent decline in amplitude of hippocampal theta oscillation was observed in response to brainstem stimulation, and the reduced hippocampal theta power showed a correlation with increased plaque load (Scott et al. 2012). In a subsequent study on 8-months-old 5xFAD mice, a similarly diminished power of elicited hippocampal theta oscillation was detected, together with a reduced power in gamma oscillation and a weakened theta-phase gamma-amplitude coupling (Stoiljkovic et al. 2016). Neurophysiological network activities, including theta rhythm, have been a major focus of studies of hippocampal function over decades (Buzsáki 2002). Hippocampal theta oscillation has been linked to various cognitive processes, and correlations between memory formation and hippocampal theta have been demonstrated in both experimental animals and humans (Buzsáki 2002; Vertes 2005; Lisman and Redish 2009; Lega et al. 2012). Therefore, in the present study, we evaluated hippocampal theta oscillation and theta-phase gamma-amplitude coupling in response to brainstem stimulation, which can provide an insight to synaptic functioning of hippocampus and one of its main behavior-independent inputs. In addition, hippocampal oscillatory activity and hippocampal–cortical interaction have also been studied in awake, freely-behaving WT and TgF344-AD rats.

Since significantly disrupted functional connectivity between cortical fields in Aβ transgenic mice have been recently reported (Busche et al. 2015), we studied connectivity between cortical field potentials in non-anaesthetized WT and TgF344-AD rats, with a particular emphasis on identifying pathological signals reflecting hyperexcitability. While it has been known that AD patients have an increased occurrence of epileptiform activity, recent 24-h electroencephalography (EEG) and intracranial recordings demonstrate a much higher percentage of epileptiform activity in this patient population (Vossel et al. 2016). Our recordings were done on 9–12 months old WT and TgF344-AD rats, at an age when some WT Fisher rats show high-voltage spindle activity (Riekkinen et al. 1992); therefore, we paid specific attention to this abnormal activity in both WT and TgF344-AD rats.

Clinical neurophysiological observations revealed profound alterations in EEG signals of AD patients; however, it has been challenging to identify corresponding abnormalities in transgenic animals capturing some form of AD pathology. There are remarkable similarities in neurophysiological signals associated with sensory processing between rodents and humans; therefore, neurophysiological signals related to sensory processing can provide potential translational biomarkers. In fact, some of the abnormal markers of sensory physiology associated with psychiatric disorders are broadly used in psychiatric drug discovery (Javitt et al. 2008). Importantly, auditory and visual abnormalities have been described in AD patients at early stage of the disease or in mild cognitive impairment (van Deursen et al. 2011; Stothart et al. 2015). Accordingly, in the present study we examined auditory evoked potentials, auditory gating, and auditory evoked steady-state response in WT and TgF344-AD rats, since some of these auditory responses are known to be affected in AD patients.

Materials and Methods

Animals

Experiments were performed on heterozygous TgF344-AD rats and their age-matched WT background Fischer344 littermates. Transgenic rats were obtained from Rat Resource and Research Center at the University of Missouri, while WT rats were purchased from Envigo (Indianapolis, IN). TgF344-AD rats were generated by co-injection of 2 transgenes both driven by mouse prion promoter elements: one contains the human Aβ precursor protein with the Swedish mutation (APPswe), and the other contains the human presenilin 1 with a deletion of exon 9 (PS1ΔE9). They were backcrossed for 12 generations onto Fisher344 strain, and before being used their genotype was confirmed by PCR analysis. Transgenic TgF344-AD model has been recently shown to faithfully reproduce all major pathological features of AD (Cohen et al. 2013).

A total of 50 rats, including both sexes, at the age of 6, 9, and 12 months were used in the study (TgF344-AD = 26 and WT = 24). Animals were housed in a temperature and humidity-controlled room with 12:12-h light-dark cycle, and with free access to food and water at all times. Measures were taken to minimize pain or discomfort and to reduce the number of animals used. All procedures were performed in accordance with National Institutes of Health guidelines (NIH publications no. 86-23, revised 1987) and were approved by the Institutional Animal Care and Use Committee of Yale University.

Electrophysiological Recordings

Electrophysiological recordings were carried out in anesthetized and in freely-behaving animals. For experiments under anesthesia rats were injected with urethane (1.5 g/kg) intraperitoneally, and placed in a Kopf stereotaxic frame (Tujunga, CA) on a temperature-regulated heating pad (Physitemp Instruments Inc., Clifton, NJ) set to maintain body temperature at 37–38 °C. Following surgical preparation and craniotomies above hippocampus and rostral pons, electrodes were inserted for recording of local field potentials (LFPs) from hippocampal CA1 region and for stimulation of nucleus pontis oralis (nPO). LFPs were recorded using a 16-site silicon recording electrode (A1 × 16-10 mm-100–177-T15; NeuroNexus Technologies, Inc, Ann Arbor, MI) positioned 3.0 mm posterior and 2.0 mm lateral to bregma, and slowly lowered 2.5–3.0 mm from the cortical surface to span the dorsal hippocampus. For electrical stimulation of the nPO, a bipolar concentric stainless steel electrode (NE-100X, Rhodes Medical Instruments, Woodland Hills, CA) was placed 7.8 mm posterior and 1.8 mm lateral to bregma, and 6.0 mm ventral from the cortical surface. Coordinates for each target area were taken from stereotaxic atlas (Paxinos and Watson 1998). Each recording began 30 min following placement of the electrodes. nPO stimulation, consisting of a train of 0.3 ms square pulses at 250 Hz over 6 s, was delivered every 100 s by an Isoflex stimulus-isolator (A.M. P.I. Instruments, Jerusalem, Israel). The stimulating current was increased stepwise from 0.0 mA to 0.2 mA in 0.02 mA increments and repeated in 2 cycles in order to establish a stimulus–response relationship for both total power and peak frequency in theta band. Throughout the duration of the experiment, rats were kept in the stereotaxic frame, spontaneous and stimulation-induced hippocampal LFPs were continuously monitored, and the level of anesthesia regularly checked.

Experiments in freely-behaving conditions were performed in male rats implanted with chronically indwelling electrodes. After achieving a surgical plane of anesthesia (mixture of 60 mg/kg ketamine and 10 mg/kg xylazine, given intraperitoneally), rats were placed in stereotaxic frame, skin shaved and cleaned, and skull exposed. Stainless steel screw electrodes were inserted under aseptic conditions over the frontal (1.0 mm anterior and 2.0 mm lateral to bregma), primary auditory (5.0 mm posterior and 4.5 mm lateral to bregma), and occipital (6.5 mm posterior and 3 mm lateral to bregma) cortices, and a deep monopolar electrode (Plastics One, Roanoke, VA) was implanted into the CA1 region of the contralateral hippocampus using coordinates as above. To serve as ground and reference, an additional 2 screws were placed over the cerebellum. All electrodes were joined to a miniature connector which was fixed to the skull using dental acrylic, and the skin incision was sutured. After surgery, each rat was put in a clean cage and all necessary postoperative care was taken. During the postsurgical recovery, one rat from each genotype lost its headset, thus leaving 5 animals in each group for further experiments. All electrophysiological recordings were carried out after 10-day recovery period, simultaneously in groups of 2 rats (one TgF344-AD and one WT) in their own home cages, and repeated weekly during light phase (between 10 a.m. and 2 p.m.). For every recording session, rats were connected to a slip-ring commutator using stainless steel spring protected cables, their cages placed in recording boxes, and left to accommodate for at least 30 min prior recordings.

At the conclusion of all acute and chronic recordings, animals were deeply anesthetized, and transcardially perfused. Brains were removed and fixed for verification of electrode placement and histological analyses.

Data Acquisition and Analyses

In each experiment, LFPs were amplified and filtered between 1 Hz and 300 Hz using A-M System (Carlsborg, WA, USA) with an additional notch filter at 60 Hz. The signal was simultaneously sampled at 2 kHz rate and stored on a computer via a CED Micro1401-3 interface and Spike2 software (Cambridge Electronic Design, Cambridge, UK). All analyses were performed with Matlab (Mathworks, Natick, MA). All offline filtering was done using the EEGLAB toolbox (Delorme and Makeig 2004).

For nPO stimulation-induced hippocampal oscillations, the first second of each 6-s long stimulation period was omitted for all analyses to avoid possible stimulation artifacts. Absolute theta power (3–9 Hz) and peak theta frequency were determined at each stimulation intensity and averaged over the 3 channels with highest LFP amplitude for each animal. Once the stimulus intensity which elicits the highest theta power was determined, each animal was subsequently stimulated with constant current in order to estimate coupling between elicited theta and gamma oscillations in the hippocampus as described earlier (Tort et al. 2009; Stoiljkovic et al. 2016).

In freely-behaving condition, 30 min of undisturbed recordings were used for all analyses. In hippocampal recordings, theta oscillations were identified as when instantaneous theta (3–12 Hz) power exceeded twice instantaneous delta (2–4 Hz) power for 2.5 s or longer, and average theta power was calculated for each. Sharp-wave ripples (SWRs) were identified as when the bandpass filtered (100–250 Hz) signal envelope exceeded the mean plus 4 times the standard deviation of the envelope for 30–150 ms, excluding instances where the signal exceeded 3 mV or when theta/delta power ratio was >2. SWR power and slow gamma power (30–50 Hz) were calculated for each event via bandpass filtering and Hilbert transform. Phase locking between frontal and occipital cortices and between frontal cortex and hippocampus during spontaneous activity were assessed by averaging phase-locking values (PLV; Lachaux et al. 1999; Mormann et al. 2000) in 20 contiguous 10-s long epochs in each behaving rat. Automatic detection of high-voltage spindles (HVSs) were identified in the frontal cortex LFP when rhythmic negative deflections lower than −0.3 mV occurred while instantaneous power between 6 Hz and 12 Hz was more than double instantaneous delta power for 2 s or longer. When SWR were identified as coincident with a HVS, the cross-correlation and Pearson's linear correlation coefficient were calculated between the LFPs in hippocampus and frontal cortex.

Auditory evoked potentials (AEPs) and auditory steady-state responses (ASSR) were recorded from primary auditory cortex in the same cohort of animals (TgF344-AD = 5, WT = 5). Auditory gating was determined using the same pattern of auditory stimulation that is used in clinical practice: delivery of 2 consecutive tone bursts (at 5 kHz) of 10 ms duration with an intertone interval of 0.5 s (Hajós 2006). AEPs were measured as the potential difference between the positive and negative deflection at 5–30 ms and 40–60 ms, respectively (P20-N40). The ratio between the AEPs of the second and first stimuli (S2/S1) was used as a measure of gating. Latency of AEP to the S1 was also analyzed. For ASSR, rats were exposed to 120 repetitions of a 3-s train consisted of 3-ms clicks at 85 db delivered at 40 Hz with 10-s intervals between trains. Average changes in power from baseline and inter-trial phase coherence (ITPC) (Tallon-Baudry et al. 1996) during stimulation were calculated from event-related potentials for each animal. Comparisons in elicited power and ITPC were made using the average of each at 40 Hz during stimulation for every animal. For both auditory assays, clicks were generated using DAQ board (model USB-6343) controlled by LabVIEW software (National Instruments, Austin, TX) and speaker mounted directly above each rat's recording box.

All data were initially determined to be suitable for parametric analysis according to normality and homoscedasticity. Statistical differences in the relationship between elicited theta power or peak frequency and current intensity were assessed by 2-way ANOVA and post hoc Bonferroni test. Changes in all other metrics tested were assessed with 2-tailed *t*-test. Data are expressed as the mean ± standard error of the mean, and differences were considered significant when $P < 0.05$.

Results

Age-Dependent Decline of Elicited Hippocampal Oscillations in Anesthetized TgF344-AD Rats

In order to characterize hippocampal network functional integrity in relation to age and strain, hippocampal oscillations elicited by electrical stimulation of the nPO were analyzed in 6- (TgF344-AD = 6; WT = 6), 9- (TgF344-AD = 7; WT = 8), and 12-month-old (TgF344-AD = 6; WT = 5) rats under anesthesia. In both rat strains, high-frequency stimulation of the nPO elicited field potential oscillations in theta range (3–9 Hz) across the hippocampal formation (Fig. 1A; Supplementary Fig. 1), with a current-dependent increase of peak frequency.

Quantitative input–output analysis of elicited theta oscillation revealed age-dependent decline in both power and peak frequency in the TgF344-AD rats when compared with their WT counterparts (Fig. 1B, Supplementary Fig. 1). At the age of

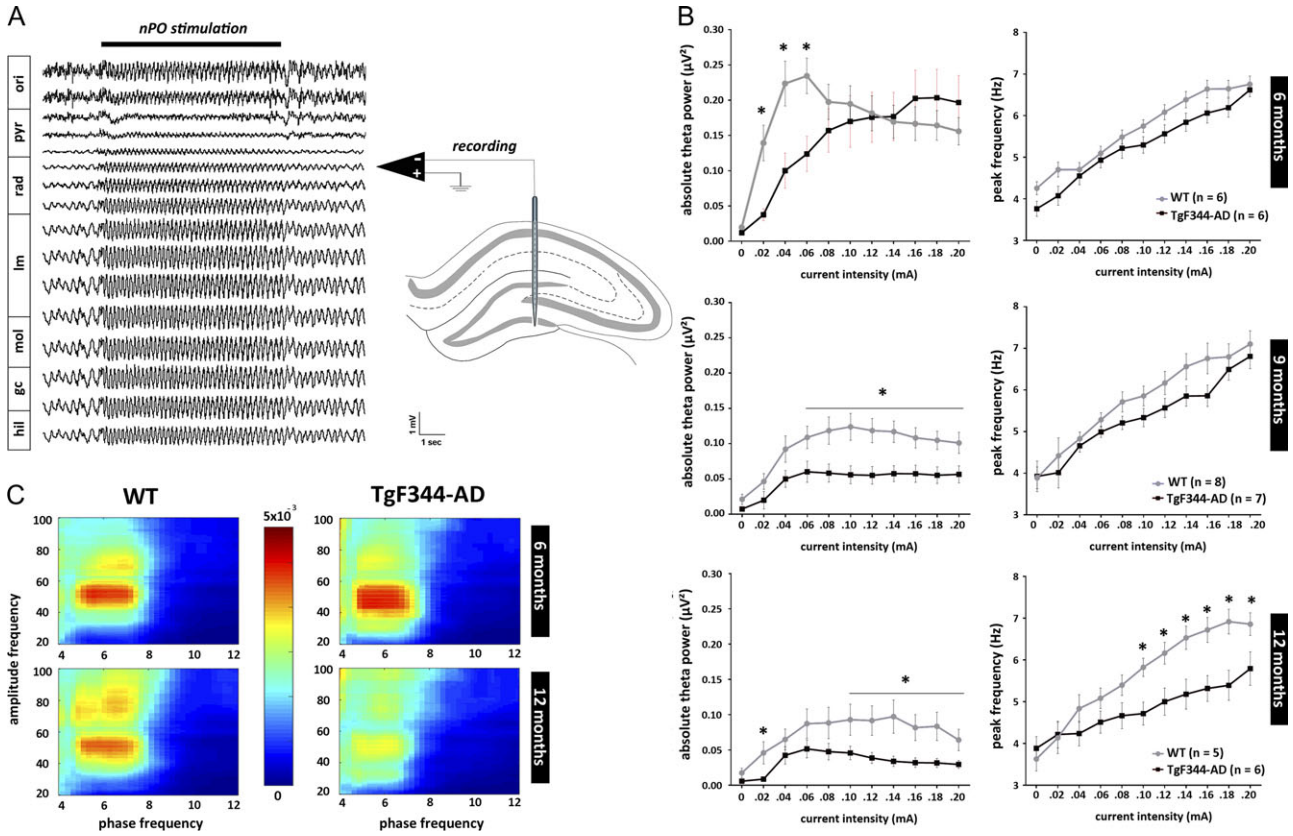

Figure 1. Age-dependent disruption of elicited hippocampal oscillations in anesthetized TgF344-AD rats. High-frequency electrical stimulation of brainstem nucleus pontis oralis (nPO) induces highly regular theta oscillations in the hippocampal CA1 region (horizontal black bar marks the period of stimulation). Local field potentials were recorded using a multi-site silicon recording electrode implanted to span the dorsal hippocampus in urethane anesthetized rats. Absolute theta power (3–9 Hz) and peak theta frequency were determined for each stimulation period using fast Fourier transformation. The average of these measures calculated from the 3 channels showing strongest theta was used for each animal. (*A*) Typical stimulation-induced theta oscillation recorded from a WT rat. Approximate reconstruction of recording sites location is based on dorso-ventral position of the electrode and observations of highest theta power in lacunosum-moleculare (Buzsáki 2002). (*B*) Stimulus–response curves created by plotting the theta power and peak frequency over increasing stimulus intensities showed age-dependent decline in both theta power and frequency in TgF344-AD rats (*$P < 0.05$). (*C*) Elicited hippocampal theta and gamma oscillations showed high theta-phase gamma-amplitude coupling as expressed by Modulation index. Phase-amplitude coupling is significantly reduced in aged TgF344-AD rats ($P < 0.05$). Abbreviations: ori—str. oriens; pyr—pyramidal layer; rad—str. radiatum; lm—str. lacunosum-moleculare; mol—molecular layer; gc—granule cell layer; hil—hilus.

6-months TgF344-AD rats showed a trend toward reduction in theta power with significant decrease in absolute power in lower theta range, but similar peak theta frequency increase over stimulus intensities ($F_{(1,22)} = 4.043$, $P = 0.057$, for theta power; $F_{(1,22)} = 0.637$, $P = 0.433$, for theta frequency). A clear decline of elicited hippocampal oscillation in TgF344-AD rats was observed at the age of 9-months, when absolute power was markedly decreased in broader theta band range ($F_{(1,28)} = 9.578$, $P < 0.005$, for theta power; $F_{(1,28)} = 2.163$, $P = 0.152$, for theta frequency). This decline was more pronounced in 12-month-old TgF344-AD rats, where both theta power and frequency were significantly reduced in comparison to their respective WT controls ($F_{(1,20)} = 5.790$, $P < 0.03$, for theta power; $F_{(1,20)} = 5.101$, $P < 0.05$, for theta frequency). No gender differences in response to nPO stimulation were observed in rats of either genotype. Interestingly, age-related decrease in hippocampal power was also noticed in WT rats. Nevertheless, overall decline in elicited hippocampal oscillations in TgF344-AD rats was more robust and accelerated with age, which is in line with previous findings in similar Aβ overproducing mouse models (Scott et al. 2012; Stoiljkovic et al. 2016).

In further assessment of elicited hippocampal oscillations, phase-amplitude coupling between theta and gamma bands was calculated. Similarly to our previous observations in anesthetized mice (Stoiljkovic et al., 2016), 2 visibly distinct bands of coupling between hippocampal theta and gamma were detected: low gamma (30–55 Hz) and high gamma (65–95 Hz). While comparable at the age of 6 months (Fig. 1C, upper heat-maps), theta-phase gamma-amplitude coupling was attenuated in both low and high gamma bands in 12-months TgF344-AD rats when compared with WT counterparts ($P < 0.05$; Fig. 1C, lower heat-maps).

Altered Hippocampal Oscillatory Activity and Long-Range Connectivity in Freely-Behaving TgF344-AD Rats

Cortical and hippocampal electrophysiological recordings were performed in non-anesthetized, freely-behaving condition in sets of animals ($n = 5$, for each genotype) in the period between 9 and 12 months of age, with some signals recorded repeatedly over this time. During awake state, evident alterations in both cortical and hippocampal oscillatory patterns were observed in TgF344-AD rats in comparison to their WT controls (Fig. 2, Supplementary Fig. 2). In particular, we found reduced hippocampal theta activity in TgF344-AD rats, with total of 393 theta oscillation events identified comparing to 708 in WT rats.

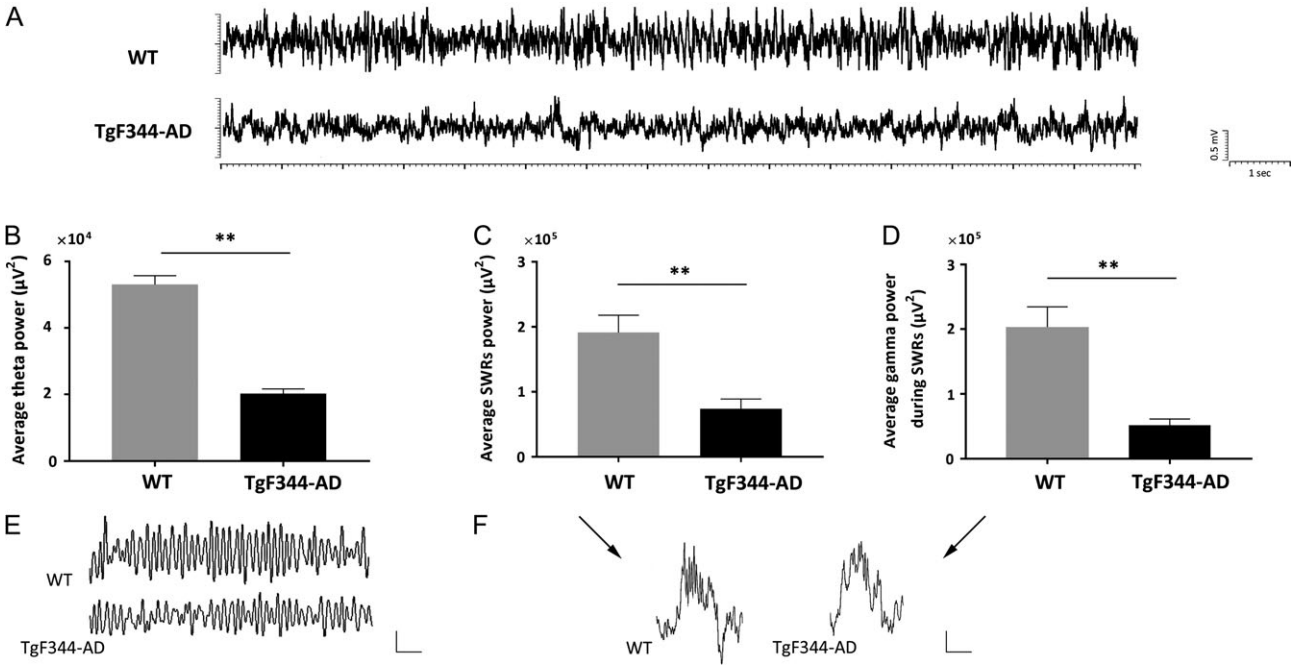

Figure 2. Reduced hippocampal oscillatory activity in non-anesthetized TgF344-AD rats. (*A*) Example of unfiltered traces of hippocampal CA1 LFP from freely-behaving WT and TgF344-AD rats. Significantly reduced power of (*B*) theta oscillations, (*C*) sharp-wave ripples (SWRs, 100–250 Hz), and (*D*) low gamma band (30–50 Hz) during SWRs in TgF344-AD rats compared with their WT controls. (**$P < 0.001$). Examples of (*E*) theta oscillation (filtered between 3 Hz and 12 Hz), and (*F*) SWR (unfiltered) traces; scale bars: 0.5 mV, 1 s for the theta traces; 0.1 mV, 0.1 s for the SWR.

Moreover, the average power of theta oscillations in TgF344-AD was significantly reduced ($P < 0.001$; Fig. 2*B*, *E*). Additionally, fewer sharp-wave ripples (SWRs, 100–250 Hz) were identified in awake TgF344-AD rats ($n_{events} = 35$) than in their WT counterparts ($n_{events} = 67$). During SWRs, the power between 100 Hz and 250 Hz and low gamma band power (30–50 Hz) were also found to be significantly reduced in TgF344-AD rats ($P < 0.001$ for both metrics; Fig. 2*C*, *D*, *F*).

Long-range connectivity was assessed using PLV (see Methods). PLV was calculated between oscillations recorded from frontal-occipital cortices and frontal cortex-contralateral hippocampus. In both cases, PLV was significantly reduced in TgF344-AD rats. More specifically, frontal-occipital cortical PLV is significantly reduced at 6–9 Hz, while cortical-hippocampal PLV is significantly reduced at 8–11 Hz and 21–31 Hz ($P < 0.05$; Fig. 3).

Increased Occurrence of Hypersynchronous High-Voltage Spindles and Weakened Interaction Between Cortical Spindles and Hippocampal Ripples in TgF344-AD Rats

Chronic cortical EEG recordings in freely-behaving TgF344-AD rats revealed numerous highly synchronous paroxysmal oscillatory bursts of large amplitude spikes with negative polarity which disrupt regular activity. This distinct oscillatory pattern, defined as high-voltage spindles (HVSs), was present in all TgF344-AD rats in each recording session over the course of 2–3 months, and very rare in WT rats. HVS episodes consisted of rhythmic spike discharges of variable duration (3.5 s on average), with frequency peak at 7–8 Hz and associated harmonics in their power spectra. They appeared spontaneously, isolated or in clusters, and exhibiting wax and wane pattern (Fig. 4*A*). The amplitude of HVSs was usually higher in the frontal than in the parietal region and diminished in the occipital region, where in most cases they were barely if at all detectable. Direct observation during recordings found that HVSs occurred only when rats were in the state of passive wakefulness (i.e., motionless but with their eyes opened). This is in agreement with previous studies where similar HVS events were reported in aged rats as well as in genetic absence-like epileptic models (Buzsáki et al. 1988; Coenen and Van Luijtelaar 2003; Shaw 2007). A total of 50 HVS events were identified in TgF344-AD rats while 6 were found in WT rats. Statistical comparison of probability of occurrence of spontaneous HVSs between TgF344-AD and age-matched WT rats calculated for each animal over a 15-min period revealed significantly greater incidence of HVSs in transgenic rats ($P < 0.001$; Fig. 4*B*). However, the pattern and average duration of HVS episodes between 2 animal groups did not significantly differ (Fig. 4*C*).

In further analysis, we investigated whether the HVSs impact interaction between cortical and hippocampal activity during SWRs in TgF344-AD rats. This was examined by calculating the cross-correlation and correlation coefficient of hippocampal and frontal cortex oscillations when SWRs and HVSs occurred simultaneously. Figure 5 shows an example of the cross-correlation during coincident events in both a WT and TgF344-AD rat, as well as a significant difference ($P < 0.001$) between the correlation coefficients pooled across all coincident events ($n_{events} = 5$ in WT; $n_{events} = 7$ in TgF344-AD).

Impaired Sensory Information Processing in TgF344-AD Rats (Auditory Evoked Potentials, Auditory Gating, ASSR)

Auditory sensory processing in TgF344-AD and WT rats was examined by measuring AEP, auditory gating, and ASSR. The magnitude of AEPs showed no significant differences between

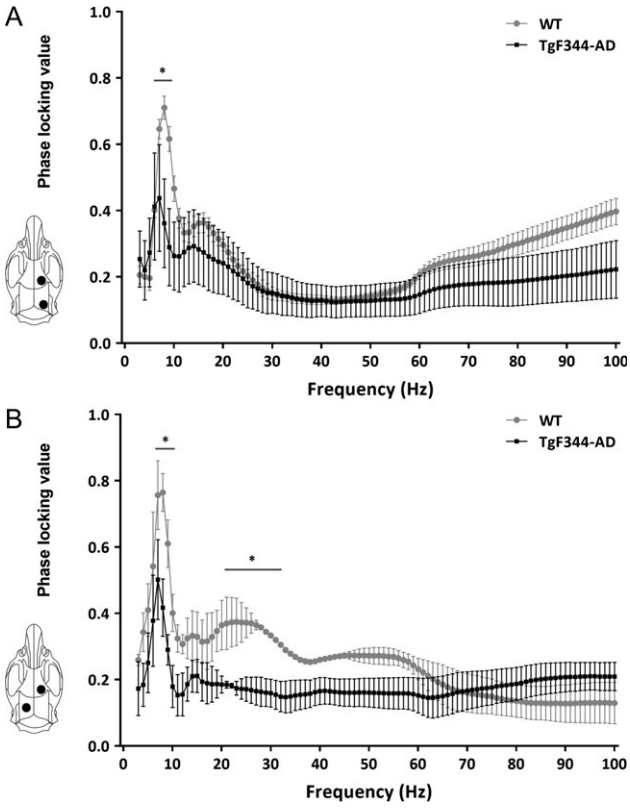

Figure 3. Disrupted temporal coordination of cortical and hippocampal oscillatory activity in TgF344-AD rats. (*A*) Functional connectivity between frontal cortex and ipsilateral occipital cortex, and (*B*) frontal cortex and contralateral hippocampus, were assessed by averaging phase-locking value (PLV) in 20 contiguous 10-s long epochs in each behaving rat. Comparing to WT rats ($n = 5$), TgF344-AD rats ($n = 5$) showed significantly lower frontal-occipital PLV at 6–9 Hz, and frontal-hippocampal PLV at 8–11 Hz and 21–31 Hz frequencies. (*$P < 0.05$).

WT and TgF344-AD rats to either the first or second stimuli, although transgenic rats showed a tendency towards reduction in the amplitude of the first stimulus. Interestingly, the latency of the AEP to the first stimulus was longer, on the borderline of significance in TgF344-AD rats ($P = 0.051$). Even though no significant difference in the absolute value of AEPs between 2 groups was observed, TgF344-AD rats showed a higher S2/S1 ratio, demonstrating significantly lower level of auditory gating in the auditory cortex ($P < 0.05$; Fig. 6). Repetitive auditory stimuli applied at 40 Hz (ASSR, see Methods for details) evoked increased power at the stimulating frequency in the auditory cortex of both TgF344-AD and WT rats. However, the 40-Hz evoked power was significantly reduced in the TgF344-AD rats compared with WT controls ($P < 0.05$; Fig. 7A). In contrast, rats from both groups showed similar ITPC in response to the 40-Hz stimuli (Fig. 7B).

Discussion

In this study, we explored hippocampal and cortical oscillatory network activities in anesthetized and freely-behaving TgF344-AD rats, a recently developed transgenic model with a full array of AD pathological features. We identified a number of neurophysiological abnormalities previously undescribed in transgenic AD models, including significantly higher occurrence of cortical HVSs, impaired interaction between HVSs and SWRs, and diminished 40-Hz ASSR-evoked power, together with anomalies already observed in Aβ overproducing mice.

Numerous studies have consistently demonstrated abnormal hippocampal morphology and function in AD patients, including a reduction in volume and irregular activation during cognitive tasks (Frisoni et al. 2010; Han et al. 2012). In line with these clinical observations, translational research in transgenic animal models of AD pathology provides various examples of hippocampal dysfunction, particularly oscillatory abnormalities. Current evidence suggests that accumulation of Aβ and hyperphosphorylated tau, major hallmarks of AD, is associated with complex disturbances in synaptic and neuronal function leading to impairments of coordinated activity in the neuronal networks that support memory and cognition (Selkoe 2002; Palop and Mucke 2016). Alterations in neuronal network activity can range from subtle changes in rhythmic activity, likely present before presentation of cognitive deficits, to profound pathology of EEG signals as disease progresses. Accordingly, impairment of hippocampal theta oscillation, considered to underlie compromised hippocampal-dependent cognitive function in transgenic APP/PS1 mice, precede their behavioral deficits (Howlett et al. 2004; Villette et al. 2010; Scott et al. 2012). Moreover, we reported that this impairment in theta oscillation is age-dependent, and its severity correlates with Aβ plaque load in the hippocampus of APP/PS1 mice (Scott et al. 2012). Consistent with these observations, our recent studies showed that both tauopathy model Tg4510 mice (Scott et al. 2016), and Aβ overproducing 5xFAD mice (Stoiljkovic et al. 2016) have significantly reduced theta power, but not peak theta frequency, during stimulation-induced hippocampal oscillations. Using the same experimental method, we found that TgF344-AD rats also show robust age-dependent reduction of elicited hippocampal theta power. Similar to aforementioned studies, theta power decline in these rats was observed by 6 months of age, before showing hippocampal-dependent learning and memory deficits (Cohen et al. 2013). Unlike our observations in mice, 12-month-old rats display a significant decline in peak theta frequency, which implies greater dysfunction of local oscillatory activity in the hippocampal network of aged TgF344-AD rats. It is noteworthy that aged WT rats also had reduced elicited theta power, which might correspond with the reported general decline in cognitive abilities of Fisher strain (Sherman et al. 1981). Furthermore, we observed diminished theta-phase gamma-amplitude coupling in the hippocampus of aged TgF344-AD rats. Coupling between the phase of theta and the amplitude of gamma oscillations has recently been demonstrated to play a critical role in supporting cognitive processes and memory formation in humans (Axmacher et al. 2010), monkeys (Canolty et al. 2010), and rodents (Tort et al. 2009; Wulff et al. 2009; Belluscio et al. 2012). Interestingly, in Aβ overproducing mice, diminished hippocampal theta-phase gamma-amplitude coupling has been shown in both *in vitro* (Goutagny et al. 2013), and *in vivo* conditions (Gurevicius et al. 2013; Stoiljkovic et al. 2016). Our current results complement and extend these observations, as TgF344-AD rats showed a significant and age-dependent deficiencies in hippocampal theta-gamma coupling, both in low and high gamma bands, when compared with younger transgenic rats or age-matched WT controls. This is also in accordance with recent studies on TgF344-AD rats (Joo et al. 2017; Bazzigaluppi et al. 2018) in which theta-gamma coupling was analyzed using resting-state oscillations in different cognitive-related brain regions.

Profound alterations in hippocampal oscillatory activity in TgF344-AD rats were also found in awake, freely-behaving conditions. Compared with WT controls, transgenic rats

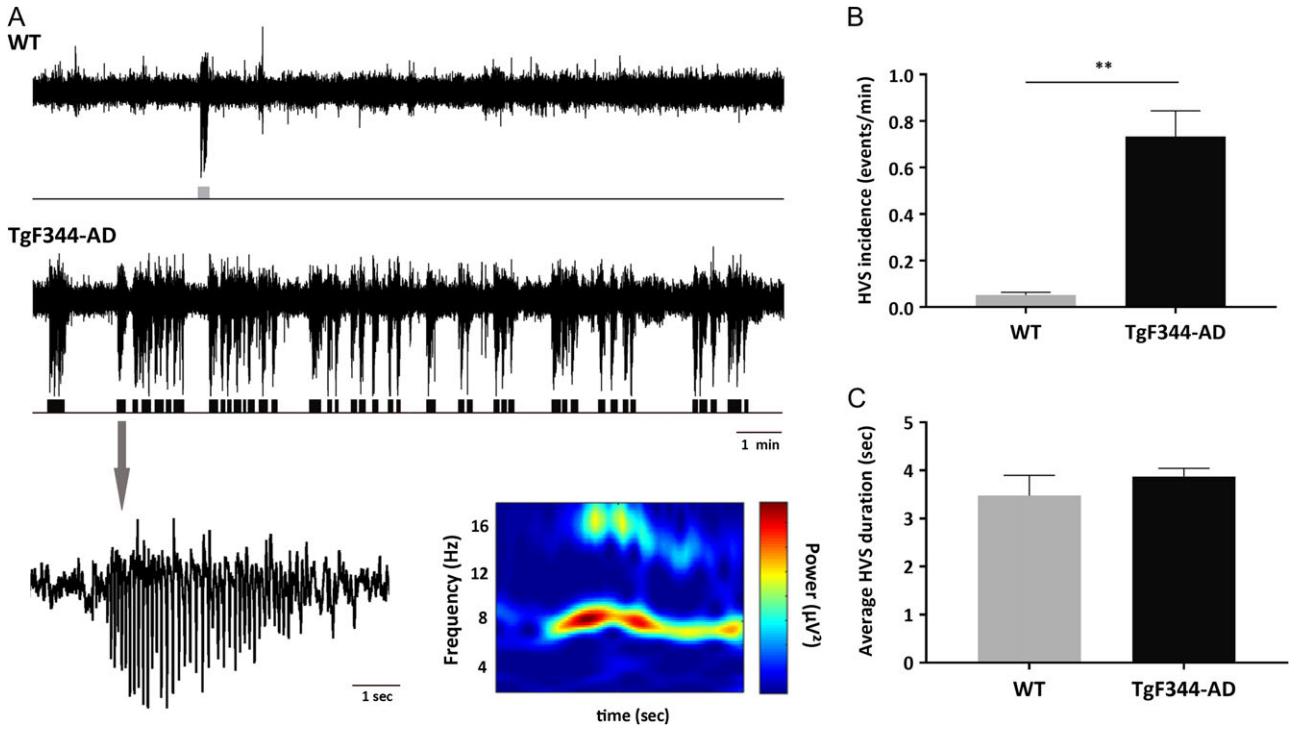

Figure 4. Altered cortical excitability in TgF344-AD rats. During awake but idling behavior spontaneously occurring high-voltage spindles (HVSs) characterized as hypersynchronous, negative voltage 7–8 Hz spike–wave discharges were observed in the cortical EEG of both WT and TgF344-AD rats. (*A*) HVSs isolated or in clusters, exhibited a wax and wane pattern, and were particularly pronounced in frontal cortex (upper and middle traces). Bottom is an enlargement of single HVS event and its corresponding time-frequency spectrogram. (*B*, *C*) In comparison to WT rats ($n = 5$), TgF344-AD rats ($n = 5$) showed significantly higher incidence of HVS events, however, the pattern and duration of HVS events did not differ, (**$P < 0.001$).

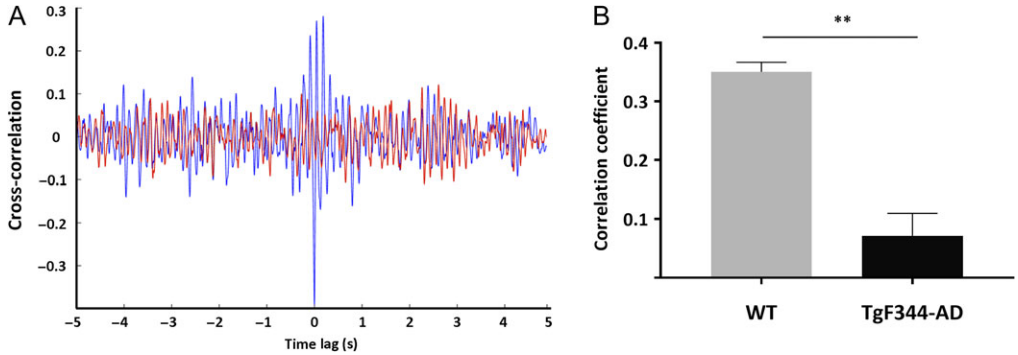

Figure 5. Reduced interaction between coincidental cortical HVSs and hippocampal SWRs in TgF344-AD rats. (*A*) Representative spindle-ripple cross-correlation for WT (blue) and TgF344-AD rat (red). In WT rats 7.5% of SWRs were coincident with HVSs, while in TgF344-AD rats 20% of SWRs were coincident with HVSs. (*B*) Correlation coefficient computed for all coincident events in every animal showing significant difference between 2 rat strains. (**$P < 0.001$).

demonstrated significantly diminished power in spontaneous theta oscillations. Furthermore, SWRs, another highly synchronous, high-frequency (100–250 Hz) hippocampal oscillation associated with cognitive function, were also impacted in TgF344-AD rats. SWRs emerge mainly during slow-wave sleep in order to strengthen and reorganize memory traces, and during passive wakefulness supporting behavioral planning (Girardeau and Zugaro 2011; Buzsáki 2015). Accordingly, increases in SWR events have been registered after learning both in humans (Axmacher et al. 2008) and rats (Ego-Stengel and Wilson 2010), while selective SWRs suppression during post-training consolidation resulted in impairment of spatial memory performances (Girardeau et al. 2009; Ego-Stengel and Wilson 2010). However, very little is known about the impact of dementia-related pathology on hippocampal SWRs. Our current findings in TgF344-AD rats demonstrate reduced SWR power accompanied by reduced power in low-frequency gamma bands. In line with our observations, disrupted SWR dynamics, with decreased amplitude and altered temporal structure have been reported in transgenic Tg4510 mice (Witton et al. 2016). Also, soluble Aβ oligomers injected intracerebroventricularly in C57BL/6 mice abolished learning-induced SWRs and impaired spatial memory (Nicole et al. 2016). Additionally, the reduction in gamma power during SWRs in TgF344-AD rats observed in this study complement similar findings reported in 5xFAD mice (Iaccarino et al. 2016). Low-frequency gamma is associated with

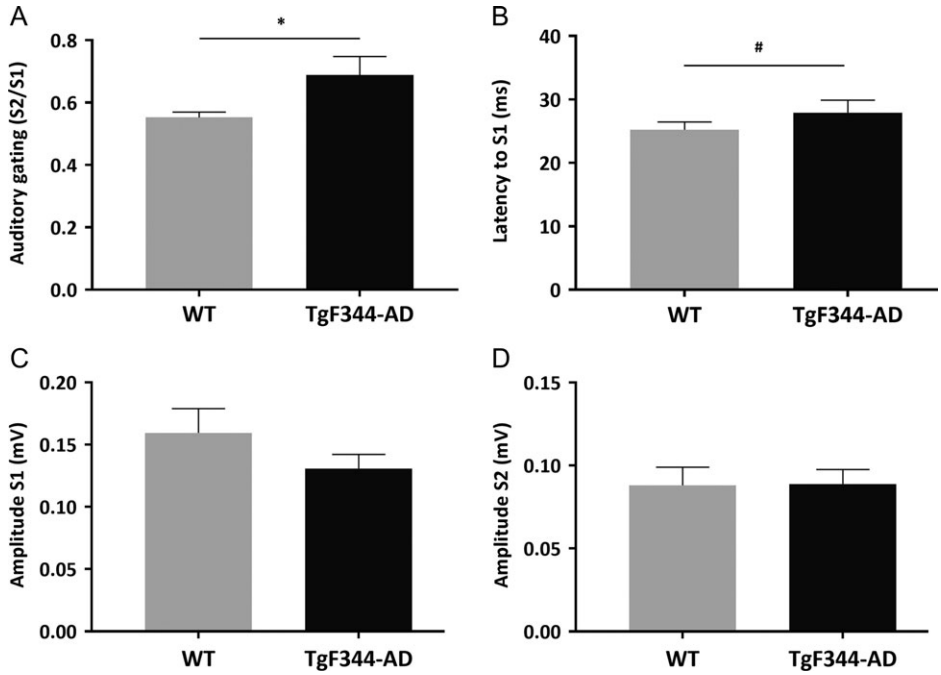

Figure 6. Auditory evoked potentials in freely-behaving WT (n = 5) and TgF344-AD (n = 5) rats were measured in the primary auditory cortex as potential difference between the positive and negative deflection at 5–30 ms and 40–60 ms, respectively (P20-N40). The ratio between the second and first stimuli (S2/S1) is used as a measure of gating. TgF344-AD rats showed (*A*) significantly impaired gating ($^{*}P < 0.05$), and (*B*) suggests prolonged latency to the first stimulus ($^{\#}P = 0.051$). (*C*, *D*) No significant difference has been observed in S1 and S2 amplitude between WT and TgF344-AD rats.

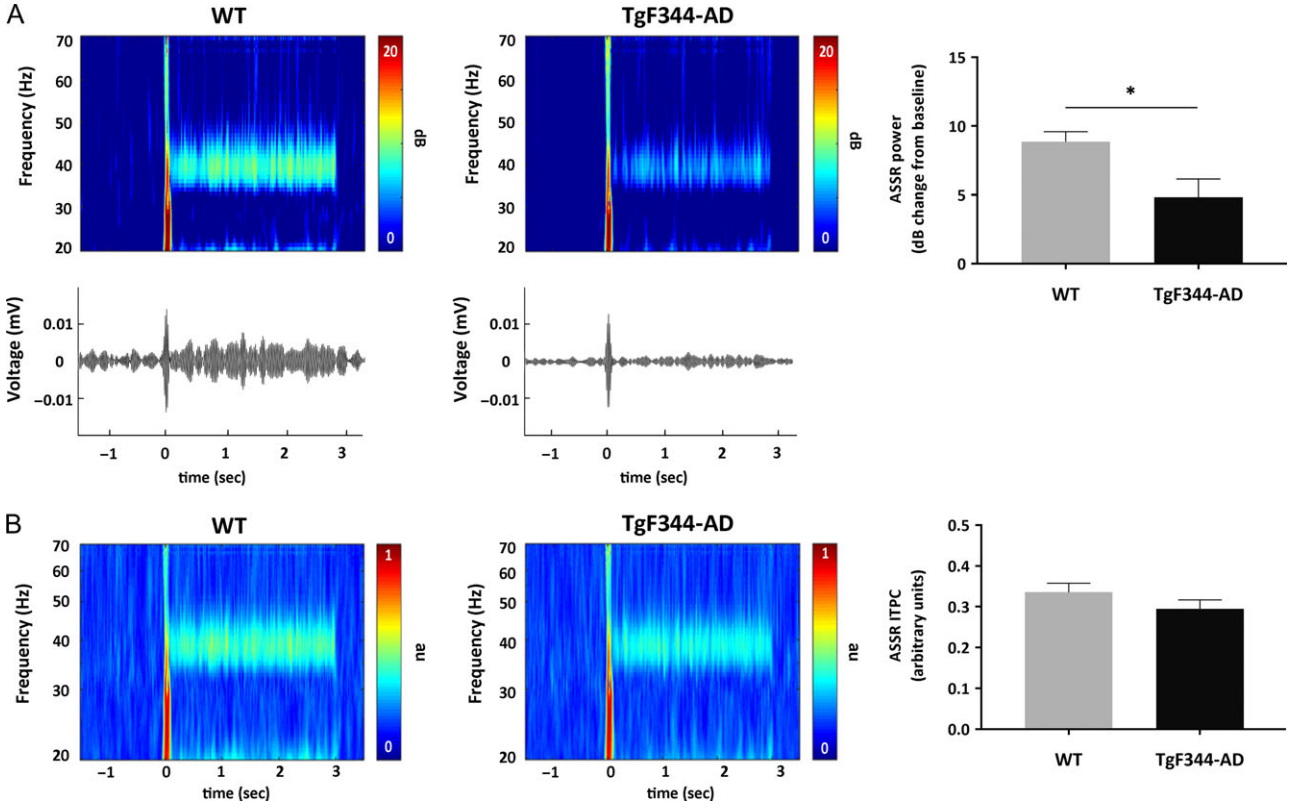

Figure 7. Auditory steady-state responses (ASSR) at 40 Hz were recorded from primary auditory cortex in freely-behaving WT (n = 5) and TgF344-AD (n = 5) rats. Output measures include 40 Hz evoked power and intertrial phase coherence (ITPC). (*A*) Time course group averages revealed decrease of the specific ASSR-evoked power in TgF344-AD rats ($^{*}P < 0.05$). Lower panels show example event-related potentials from a single WT and TgF344-AD rat. (*B*) No significant changes have been observed in ITPC between WT and TgF344-AD rats.

gamma locking between CA3 and CA1 (Colgin et al. 2009), regions where SWRs emerge. Since gamma oscillation critically depends on GABAergic interneuron function, our results might indicate that interneurons involved in neural circuits associated with learning and memory are particularly affected by AD pathologies. In fact, dysfunction of GABAergic interneurons is considered a critical contribution to AD pathology (Palop and Mucke 2016).

Dynamic functional connectivity within and between distributed brain regions such as the cortex and hippocampus has been demonstrated to be necessary for normal cognitive processing (reviewed in Bressler and Menon 2010). Therefore, disruption of functional connectivity is considered an important biomarker for cognitive deficits (Zhang and Raichle 2010; Bero et al. 2012). Hence, we measured phase locking between spontaneous oscillations from the frontal and occipital cortical regions, as well as from frontal and hippocampal regions, in freely-behaving rats. We found decreases in the theta band in cortico-cortical and in theta and beta bands in cortico-hippocampal connectivity in TgF344-AD rats relative to WT controls. It has been postulated that during cognitive processing, theta rhythm facilitates the formation of long-range functional networks (Buzsáki and Draguhn 2004). These findings align with previous observations in which AD progressively affected and impaired long-range connections in the cortex and hippocampus in both patients and transgenic mice (Buckner et al. 2009; Bero et al. 2012; Busche et al. 2015; Babiloni et al. 2016).

The most striking alteration seen in TgF344-AD rats, however, was the immensely high rate of occurrence of spontaneous HVSs in the cortical EEG. These hypersynchronous 7–8 Hz spike–wave discharges were present in both TgF344-AD and age-matched WT rats during passive wakefulness; however, their incidence was roughly 15-fold greater in transgenic rats. HVSs were previously described in aged rats of several strains (Buzsáki et al. 1988; Radek et al. 1994). They are assumed to reflect epileptic absence seizures based on their spike and wave pattern, unresponsiveness to mild stimuli, and reduction by antiabsence drugs (Shaw 2007). Spontaneous nonconvulsive seizures have been also described in different lines of transgenic Aβ overproducing mice (Palop et al. 2007; Minkeviciene et al. 2009), and more importantly in AD patients (Born 2015; Vossel et al. 2017). An early study showed that increase in HVS events coincided with spatial memory deficits in rats (Radek et al. 1994). This is in line with the proposed causal relationship between spontaneous recurrent seizures and impairments in cognitive functions in mouse models of AD (Palop et al. 2007; Chin and Scharfman 2013), and could possibly explain the poor spatial memory performance of TgF344-AD rats (Cohen et al. 2013). Interestingly, some findings indicate that increases in neuronal activity, such as during seizures, can exacerbate Aβ and tau pathology (Yamamoto et al. 2015; Wu et al. 2016). Additionally, new data raise the possibility that clinically silent neuronal hyperexcitability reflected in subclinical epileptiform activity (i.e., epilepsy-like activity in the absence of clinical seizures), recognized in early stage of disease, might accelerate cognitive decline in AD patients (Vossel et al. 2016, 2017). The exact mechanism underlying development of HVSs and their presumed role in cognitive dysfunction is not completely understood. However, previous findings indicate that impaired cholinergic neurotransmission of the nucleus basalis (NB) in basal forebrain (BF) is a likely substrate for spindling activity in neocortex (Buzsáki et al. 1988; Riekkinen et al. 1992). Cholinergic projections of NB provide activation of neocortex (Mesulam 2013), as well as tonic inhibition of the reticular nucleus of the thalamus (RT), a putative spindle pacemaker (Buzsáki et al. 1988). When the RT is released from NB inhibition due to decrease in cholinergic tone, presumably occurring as a consequence of the aging or neurodegenerative processes, it disinhibits thalamocortical relay nuclei which in turn may trigger HVS discharges.

Experimental data suggest that epileptiform activity could contribute to impairment of synaptic plasticity that leads to deficits in hippocampal memory function (Palop et al. 2007). Thus, we hypothesize that observed abundance of cortical HVSs in TgF344-AD rats may have a detrimental impact on hippocampal activity, since spindles can reach hippocampus by the neocortical-entorhinal cortex path (Rolls 2000). In fact, previous studies have established a correlation between sleep-associated spindles recorded from the somatosensory, prefrontal, and visual cortices with hippocampal SWRs (Buzsáki 2015). Furthermore, a recent study (Haggerty and Ji 2014) reported temporal reduction in hippocampal SWRs at or soon after the onset of sleep-associated cortical spindles. Here, we compared interaction between HVSs and SWRs in WT and TgF344-AD rats during periods of passive wakefulness, and found significantly reduced correlation of HVSs and SWRs in transgenic animals. Given the high incidence of HVSs expression in TgF344-AD rats, we speculate that this recurrent cortical spindling keeps hippocampal activity suppressed during resting behavior, and thus affects synaptic plasticity and memory consolidation.

In addition, TgF344-AD rats demonstrated impairments in sensory processing, exhibiting diminished auditory gating and 40 Hz ASSR response in the auditory cortex. Auditory gating deficit is thought to reflect the brain's inability to inhibit redundant information which is a precondition for efficient cognitive processing (Hajós 2006). In accordance with a previous study in APP/PS1 mice (Wang et al. 2003), we found a significant gating deficit with suggestive increase in latency to the first AEP in TgF344-AD rats. Our result is also in agreement with clinical findings (Thomas et al. 2010), where auditory gating deficit in patients with mild to moderate AD was remarkably correlated with impairment in frontal executive functions and sustained attention. It is noteworthy that auditory gating deficit is tied extensively to disturbances in cholinergic function, and can be improved with drugs that increase cholinergic tone such as donepezil, which is approved for AD therapy (Klinkenberg et al. 2013). Furthermore, significant reduction of 40 Hz evoked ASSR power in transgenic rats was detected. Interestingly, no study has yet investigated ASSR in transgenic AD models, and rare clinical data provide contradictory results showing either a decrease (Ribary et al. 1991) or increase (van Deursen et al. 2011) in response to 40 Hz ASSR. Also, there is an indication that the brain's ability to synchronize oscillations with 40 Hz ASSR stimulation decreases linearly with age (Griskova-Bulanova et al. 2013). The ASSR at 40 Hz can be strongly modulated by both cholinergic and GABAergic neurons, since blockade of cholinergic receptors in rats (Zhang et al. 2016) or selective optogenetic inhibition of fast-spiking, parvalbumin-positive GABAergic interneurons in the BF of mice (Kim et al. 2015) can significantly reduce 40 Hz evoked power. Considering that cholinergic neurons can excite cortically projecting BF GABAergic interneurons (Yang et al. 2014), as well as suggested impairments of cholinergic neuronal functions in BF over the course of aging and in AD (Mesulam 2013), reduction in ASSR power, as observed in this study, could be expected.

Compelling evidence suggests that BF cholinergic neurons are among the earliest targets of AD pathology, with abnormalities apparent before the onset of cognitive symptomatology

(Baker-Nigh et al. 2015; Schmitz et al. 2016). In TgF344-AD rats, we have observed hyperphosphorylated tau in BF cholinergic neurons (Supplementary Fig. 3), in line with previous findings of tau pathology in these rats (Cohen et al. 2013). Additionally, tau-induced alterations have also been described in fast-spiking, parvalbumin-positive GABAergic interneurons in the BF septum/diagonal band of Broca, which innervates the hippocampus and regulates its rhythmic activity (Soler et al. 2017). Under normal condition, BF cholinergic neurons and GABAergic interneurons likely coordinate to control cortical activation and provide rhythmic drive to the hippocampus. Accumulation of Aβ and hyperphosphorylated tau could disrupt multiple aspects of this coordination, leading to abnormalities in cortical and hippocampal oscillations, as observed in TgF344-AD rats. The reported abnormalities in these rats, some of which mirror alterations observed in AD patients, may be used for further understanding of the mechanisms of disease, and for evaluating the potential of novel therapeutic approaches.

Supplementary Material

Supplementary material is available at *Cerebral Cortex* online.

Funding

This work was supported by H. Lundbeck A/S and Otsuka Pharmaceuticals, and, NIH grants (AG052986, AG052986 and AG051459).

Notes

A preliminary report of these data was presented in abstract form at the World Congress of Neurology 2017, Kyoto, Japan. *Conflict of Interest*: None declared.

References

Axmacher N, Elger CE, Fell J. 2008. Ripples in the medial temporal lobe are relevant for human memory consolidation. Brain. 131:1806–1817.

Axmacher N, Henseler MM, Jensen O, Weinreich I, Elger CE, Fell J. 2010. Cross-frequency coupling supports multi-item working memory in the human hippocampus. Proc Natl Acad Sci USA. 107:3228–3233.

Babiloni C, Lizio R, Marzano N, Capotosto P, Soricelli A, Triggiani AI, Cordone S, Gesualdo L, Del Percio C. 2016. Brain neural synchronization and functional coupling in Alzheimer's disease as revealed by resting state EEG rhythms. Int J Psychophysiol. 103:88–102.

Baker-Nigh A, Vahedi S, Davis EG, Weintraub S, Bigio EH, Klein WL, Geula C. 2015. Neuronal amyloid-beta accumulation within cholinergic basal forebrain in ageing and Alzheimer's disease. Brain. 138:1722–1737.

Bazzigaluppi P, Beckett TL, Koletar MM, Lai AY, Joo IL, Brown ME, Carlen PL, McLaurin J, Stefanovic B. 2018. Early-stage attenuation of phase-amplitude coupling in the hippocampus and medial prefrontal cortex in a transgenic rat model of Alzheimer's disease. J Neurochem. 144:669–679.

Belluscio MA, Mizuseki K, Schmidt R, Kempter R, Buzsaki G. 2012. Cross-frequency phase-phase coupling between theta and gamma oscillations in the hippocampus. J Neurosci. 32:423–435.

Bero AW, Bauer AQ, Stewart FR, White BR, Cirrito JR, Raichle ME, Culver JP, Holtzman DM. 2012. Bidirectional relationship between functional connectivity and amyloid-beta deposition in mouse brain. J Neurosci. 32:4334–4340.

Born HA. 2015. Seizures in Alzheimer's disease. Neuroscience. 286:251–263.

Bressler SL, Menon V. 2010. Large-scale brain networks in cognition: emerging methods and principles. Trends Cogn Sci. 14:277–290.

Buckner RL, Sepulcre J, Talukdar T, Krienen FM, Liu H, Hedden T, Andrews-Hanna JR, Sperling RA, Johnson KA. 2009. Cortical hubs revealed by intrinsic functional connectivity: mapping, assessment of stability, and relation to Alzheimer's disease. J Neurosci. 29:1860–1873.

Busche MA, Kekus M, Adelsberger H, Noda T, Forstl H, Nelken I, Konnerth A. 2015. Rescue of long-range circuit dysfunction in Alzheimer's disease models. Nat Neurosci. 18:1623–1630.

Buzsáki G. 2002. Theta oscillations in the hippocampus. Neuron. 33:325–340.

Buzsáki G. 2015. Hippocampal sharp wave-ripple: a cognitive biomarker for episodic memory and planning. Hippocampus. 25:1073–1188.

Buzsáki G, Bickford RG, Ponomareff G, Thal LJ, Mandel R, Gage FH. 1988. Nucleus basalis and thalamic control of neocortical activity in the freely moving rat. J Neurosci. 8:4007–4026.

Buzsáki G, Draguhn A. 2004. Neuronal oscillations in cortical networks. Science. 304:1926–1929.

Canolty RT, Ganguly K, Kennerley SW, Cadieu CF, Koepsell K, Wallis JD, Carmena JM. 2010. Oscillatory phase coupling coordinates anatomically dispersed functional cell assemblies. Proc Natl Acad Sci USA. 107:17356–17361.

Chin J, Scharfman HE. 2013. Shared cognitive and behavioral impairments in epilepsy and Alzheimer's disease and potential underlying mechanisms. Epilepsy Behav. 26:343–351.

Coenen AM, Van Luijtelaar EL. 2003. Genetic animal models for absence epilepsy: a review of the WAG/Rij strain of rats. Behav Genet. 33:635–655.

Cohen RM, Rezai-Zadeh K, Weitz TM, Rentsendorj A, Gate D, Spivak I, Bholat Y, Vasilevko V, Glabe CG, Breunig JJ, et al. 2013. A transgenic Alzheimer rat with plaques, tau pathology, behavioral impairment, oligomeric abeta, and frank neuronal loss. J Neurosci. 33:6245–6256.

Colgin LL, Denninger T, Fyhn M, Hafting T, Bonnevie T, Jensen O, Moser MB, Moser EI. 2009. Frequency of gamma oscillations routes flow of information in the hippocampus. Nature. 462:353–357.

Delorme A, Makeig S. 2004. EEGLAB: an open source toolbox for analysis of single-trial EEG dynamics including independent component analysis. J Neurosci Methods. 134:9–21.

Ego-Stengel V, Wilson MA. 2010. Disruption of ripple-associated hippocampal activity during rest impairs spatial learning in the rat. Hippocampus. 20:1–10.

Frisoni GB, Fox NC, Jack CR Jr., Scheltens P, Thompson PM. 2010. The clinical use of structural MRI in Alzheimer disease. Nat Rev Neurol. 6:67–77.

Girardeau G, Benchenane K, Wiener SI, Buzsaki G, Zugaro MB. 2009. Selective suppression of hippocampal ripples impairs spatial memory. Nat Neurosci. 12:1222–1223.

Girardeau G, Zugaro M. 2011. Hippocampal ripples and memory consolidation. Curr Opin Neurobiol. 21:452–459.

Goutagny R, Gu N, Cavanagh C, Jackson J, Chabot JG, Quirion R, Krantic S, Williams S. 2013. Alterations in hippocampal network oscillations and theta-gamma coupling arise before Aβ overproduction in a mouse model of Alzheimer's disease. Eur J Neurosci. 37:1896–1902.

Griskova-Bulanova I, Dapsys K, Maciulis V. 2013. Does brain ability to synchronize with 40 Hz auditory stimulation change with age? Acta Neurobiol Exp (Wars). 73:564–570.

Gurevicius K, Lipponen A, Tanila H. 2013. Increased cortical and thalamic excitability in freely moving APPswe/PS1dE9 mice modeling epileptic activity associated with Alzheimer's disease. Cereb Cortex. 23:1148–1158.

Haggerty DC, Ji D. 2014. Initiation of sleep-dependent cortical-hippocampal correlations at wakefulness-sleep transition. J Neurophysiol. 112:1763–1774.

Hajós M. 2006. Targeting information-processing deficit in schizophrenia: a novel approach to psychotherapeutic drug discovery. Trends Pharmacol Sci. 27:391–398.

Han SD, Gruhl J, Beckett L, Dodge HH, Stricker NH, Farias S, Mungas D, Alzheimer's Disease Neuroimaging I. 2012. Beta amyloid, tau, neuroimaging, and cognition: sequence modeling of biomarkers for Alzheimer's Disease. Brain Imaging Behav. 6:610–620.

Howlett DR, Richardson JC, Austin A, Parsons AA, Bate ST, Davies DC, Gonzalez MI. 2004. Cognitive correlates of Aβ deposition in male and female mice bearing amyloid precursor protein and presenilin-1 mutant transgenes. Brain Res. 1017:130–136.

Iaccarino HF, Singer AC, Martorell AJ, Rudenko A, Gao F, Gillingham TZ, Mathys H, Seo J, Kritskiy O, Abdurrob F, et al. 2016. Gamma frequency entrainment attenuates amyloid load and modifies microglia. Nature. 540:230–235.

Javitt DC, Spencer KM, Thaker GK, Winterer G, Hajós M. 2008. Neurophysiological biomarkers for drug development in schizophrenia. Nat Rev Drug Discov. 7:68–83.

Joo IL, Lai AY, Bazzigaluppi P, Koletar MM, Dorr A, Brown ME, Thomason LA, Sled JG, McLaurin J, Stefanovic B. 2017. Early neurovascular dysfunction in a transgenic rat model of Alzheimer's disease. Sci Rep. 7:46427.

Kim T, Thankachan S, McKenna JT, McNally JM, Yang C, Choi JH, Chen L, Kocsis B, Deisseroth K, Strecker RE, et al. 2015. Cortically projecting basal forebrain parvalbumin neurons regulate cortical gamma band oscillations. Proc Natl Acad Sci USA. 112:3535–3540.

Klinkenberg I, Sambeth A, Blokland A. 2013. Cholinergic gating of hippocampal auditory evoked potentials in freely moving rats. Eur Neuropsychopharmacol. 23:988–997.

Lachaux JP, Rodriguez E, Martinerie J, Varela FJ. 1999. Measuring phase synchrony in brain signals. Hum Brain Mapp. 8: 194–208.

Lega BC, Jacobs J, Kahana M. 2012. Human hippocampal theta oscillations and the formation of episodic memories. Hippocampus. 22:748–761.

Lisman J, Redish AD. 2009. Prediction, sequences and the hippocampus. Philos Trans R Soc Lond B Biol Sci. 364: 1193–1201.

Mesulam MM. 2013. Cholinergic circuitry of the human nucleus basalis and its fate in Alzheimer's disease. J Comp Neurol. 521:4124–4144.

Minkeviciene R, Rheims S, Dobszay MB, Zilberter M, Hartikainen J, Fulop L, Penke B, Zilberter Y, Harkany T, Pitkanen A, et al. 2009. Amyloid beta-induced neuronal hyperexcitability triggers progressive epilepsy. J Neurosci. 29:3453–3462.

Mormann F, Lehnertz K, David P, Christian E, Elger CE. 2000. Mean phase coherence as a measure for phase synchronization and its application to the EEG of epilepsy patients. Physica D: Nonlinear Phenomena. 144:358–369.

Nicole O, Hadzibegovic S, Gajda J, Bontempi B, Bem T, Meyrand P. 2016. Soluble amyloid beta oligomers block the learning-induced increase in hippocampal sharp wave-ripple rate and impair spatial memory formation. Sci Rep. 6:22728.

Palop JJ, Chin J, Roberson ED, Wang J, Thwin MT, Bien-Ly N, Yoo J, Ho KO, Yu GQ, Kreitzer A, et al. 2007. Aberrant excitatory neuronal activity and compensatory remodeling of inhibitory hippocampal circuits in mouse models of Alzheimer's disease. Neuron. 55:697–711.

Palop JJ, Mucke L. 2016. Network abnormalities and interneuron dysfunction in Alzheimer disease. Nat Rev Neurosci. 17: 777–792.

Paxinos G, Watson C. 1998. The Rat Brain in Stereotaxic Coordinates. 4th ed. San Diego: Academic Press.

Radek RJ, Curzon P, Decker MW. 1994. Characterization of high voltage spindles and spatial memory in young, mature and aged rats. Brain Res Bull. 33:183–188.

Ribary U, Ioannides AA, Singh KD, Hasson R, Bolton JP, Lado F, Mogilner A, Llinas R. 1991. Magnetic field tomography of coherent thalamocortical 40-Hz oscillations in humans. Proc Natl Acad Sci USA. 88:11037–11041.

Riekkinen P Jr., Riekkinen M, Sirvio J, Miettinen R, Riekkinen P. 1992. Loss of cholinergic neurons in the nucleus basalis induces neocortical electroencephalographic and passive avoidance deficits. Neuroscience. 47:823–831.

Rolls ET. 2000. Hippocampo-cortical and cortico-cortical back-projections. Hippocampus. 10:380–388.

Schmitz TW, Nathan Spreng R, Alzheimer's Disease Neuroimaging I. 2016. Basal forebrain degeneration precedes and predicts the cortical spread of Alzheimer's pathology. Nat Commun. 7: 13249.

Scott L, Feng J, Kiss T, Needle E, Atchison K, Kawabe TT, Milici AJ, Hajós-Korcsok E, Riddell D, Hajós M. 2012. Age-dependent disruption in hippocampal theta oscillation in amyloid-β overproducing transgenic mice. Neurobiol Aging. 33:1481 e1413–e1423.

Scott L, Kiss T, Kawabe TT, Hajós M. 2016. Neuronal network activity in the hippocampus of tau transgenic (Tg4510) mice. Neurobiol Aging. 37:66–73.

Selkoe DJ. 2002. Alzheimer's disease is a synaptic failure. Science. 298:789–791.

Shaw FZ. 2007. 7–12 Hz high-voltage rhythmic spike discharges in rats evaluated by antiepileptic drugs and flicker stimulation. J Neurophysiol. 97:238–247.

Sherman KA, Kuster JE, Dean RL, Bartus RT, Friedman E. 1981. Presynaptic cholinergic mechanisms in brain of aged rats with memory impairments. Neurobiol Aging. 2:99–104.

Soler H, Dorca-Arevalo J, Gonzalez M, Rubio SE, Avila J, Soriano E, Pascual M. 2017. The GABAergic septohippocampal connection is impaired in a mouse model of tauopathy. Neurobiol Aging. 49:40–51.

Stoiljkovic M, Kelley C, Hajós GP, Nagy D, Koenig G, Leventhal L, Hajós M. 2016. Hippocampal network dynamics in response to α7 nACh receptors activation in amyloid-β overproducing transgenic mice. Neurobiol Aging. 45:161–168.

Stothart G, Kazanina N, Naatanen R, Haworth J, Tales A. 2015. Early visual evoked potentials and mismatch negativity in Alzheimer's disease and mild cognitive impairment. J Alzheimers Dis. 44:397–408.

Tallon-Baudry C, Bertrand O, Delpuech C, Pernier J. 1996. Stimulus specificity of phase-locked and non-phase-locked 40 Hz visual responses in human. J Neurosci. 16:4240–4249.

Thomas C, vom Berg I, Rupp A, Seidl U, Schroder J, Roesch-Ely D, Kreisel SH, Mundt C, Weisbrod M. 2010. P50 gating deficit in Alzheimer dementia correlates to frontal neuropsychological function. Neurobiol Aging. 31:416–424.

Tort AB, Komorowski RW, Manns JR, Kopell NJ, Eichenbaum H. 2009. Theta-gamma coupling increases during the learning of item-context associations. Proc Natl Acad Sci USA. 106: 20942–20947.

van Deursen JA, Vuurman EF, van Kranen-Mastenbroek VH, Verhey FR, Riedel WJ. 2011. 40-Hz steady state response in Alzheimer's disease and mild cognitive impairment. Neurobiol Aging. 32:24–30.

Vertes RP. 2005. Hippocampal theta rhythm: a tag for short-term memory. Hippocampus. 15:923–935.

Villette V, Poindessous-Jazat F, Simon A, Lena C, Roullot E, Bellessort B, Epelbaum J, Dutar P, Stephan A. 2010. Decreased rhythmic GABAergic septal activity and memory-associated θ oscillations after hippocampal amyloid-β pathology in the rat. J Neurosci. 30:10991–11003.

Vossel KA, Ranasinghe KG, Beagle AJ, Mizuiri D, Honma SM, Dowling AF, Darwish SM, Van Berlo V, Barnes DE, Mantle M, et al. 2016. Incidence and impact of subclinical epileptiform activity in Alzheimer's disease. Ann Neurol. 80:858–870.

Vossel KA, Tartaglia MC, Nygaard HB, Zeman AZ, Miller BL. 2017. Epileptic activity in Alzheimer's disease: causes and clinical relevance. Lancet Neurol. 16:311–322.

Wang J, Ikonen S, Gurevicius K, Van Groen T, Tanila H. 2003. Altered auditory-evoked potentials in mice carrying mutated human amyloid precursor protein and presenilin-1 transgenes. Neuroscience. 116:511–517.

Witton J, Staniaszek LE, Bartsch U, Randall AD, Jones MW, Brown JT. 2016. Disrupted hippocampal sharp-wave ripple-associated spike dynamics in a transgenic mouse model of dementia. J Physiol. 594:4615–4630.

Wu JW, Hussaini SA, Bastille IM, Rodriguez GA, Mrejeru A, Rilett K, Sanders DW, Cook C, Fu H, Boonen RA, et al. 2016. Neuronal activity enhances tau propagation and tau pathology *in vivo*. Nat Neurosci. 19:1085–1092.

Wulff P, Ponomarenko AA, Bartos M, Korotkova TM, Fuchs EC, Bahner F, Both M, Tort AB, Kopell NJ, Wisden W, et al. 2009. Hippocampal theta rhythm and its coupling with gamma oscillations require fast inhibition onto parvalbumin-positive interneurons. Proc Natl Acad Sci USA. 106: 3561–3566.

Yamamoto K, Tanei ZI, Hashimoto T, Wakabayashi T, Okuno H, Naka Y, Yizhar O, Fenno LE, Fukayama M, Bito H, et al. 2015. Chronic optogenetic activation augments Aβ pathology in a mouse model of Alzheimer disease. Cell Rep. 11:859–865.

Yang C, McKenna JT, Zant JC, Winston S, Basheer R, Brown RE. 2014. Cholinergic neurons excite cortically projecting basal forebrain GABAergic neurons. J Neurosci. 34:2832–2844.

Zhang J, Ma L, Li W, Yang P, Qin L. 2016. Cholinergic modulation of auditory steady-state response in the auditory cortex of the freely moving rat. Neuroscience. 324:29–39.

Zhang D, Raichle ME. 2010. Disease and the brain's dark energy. Nat Rev Neurol. 6:15–28.